

Identifying Multiscale Spatio-Temporal Patterns in Human Mobility using Manifold Learning

James R. Watson¹, Zachery Gelbaum², Mathew Titus³, Grant Zoch⁴, and David Wrathall⁵

¹**College of Earth, Ocean and Atmospheric Sciences, Oregon State University**

²**College of Earth, Ocean and Atmospheric Sciences, Oregon State University**

³**College of Earth, Ocean and Atmospheric Sciences, Oregon State University**

⁴**College of Earth, Ocean and Atmospheric Sciences, Oregon State University**

⁵**College of Earth, Ocean and Atmospheric Sciences, Oregon State University**

¹¹ Corresponding author:

¹² James R. Watson¹

¹³ Email address: james.watson@oregonstate.edu

ABSTRACT

¹⁵ When, where and how people move is a fundamental part of how human societies organize around every-day needs as well as how people adapt to risks, such as economic scarcity or instability, and natural disasters. Our ability to characterize and predict the diversity of human mobility patterns has been greatly expanded by the availability of Call Detail Records (CDR) from mobile phone cellular networks. The size and richness of these datasets is at the same time a blessing and a curse: while there is great opportunity to extract useful information from these datasets, it remains a challenge to do so in a meaningful way. In particular, human mobility is multiscale, meaning a diversity of patterns of mobility occur simultaneously, which vary according to timing, magnitude and spatial extent. To identify and characterize the main spatio-temporal scales and patterns of human mobility we examined CDR data from the Orange mobile network in Senegal using a new form of spectral graph wavelets, an approach from manifold learning. This unsupervised analysis reduces the dimensionality of the data to reveal seasonal changes in human mobility, as well as mobility patterns associated with large-scale but short-term religious events. The novel insight into human mobility patterns afforded by manifold learning methods like spectral graph wavelets have clear applications for urban planning, infrastructure design as well as hazard risk management, especially as climate change alters the biophysical landscape on which people work and live, leading to new patterns of human migration around the world.

INTRODUCTION

³² Human mobility is a fundamental part of how individuals, households and communities organize to meet every-day needs, and to respond to infrequent risks and shocks like economic instability and environmental hazards. Human mobility is multiscale in nature (Song et al., 2010a), that is for any given type of mobility, such as commuting, seasonal migration or holiday travels, individuals move as part of social collectives of varying size and interconnectivity, which span different magnitudes of spatial and temporal scale. Human mobility also has multiple spatio-temporal modes of variability: people go to work each day, they go on holiday during specific programmed periods within the year, they may migrate before and after key agricultural seasons, or they may evacuate during floods or other environmental hazards (Widhalm et al., 2015). For these reasons and others, it is a continuing challenge to identify, categorize and anticipate the various patterns of human mobility (Simini et al., 2012). Anticipating and planning for human mobility is a non-trivial task for organizations whose core functions provide critical services to and address the needs of moving people, such as urban planning and transport agencies, disaster first-responders and international aid organizations (Jiang et al., 2017).

⁴⁵ To overcome these challenges and generate fundamental insight on human mobility, novel data

generated by users of the digital infrastructure (e.g. mobile phone subscribers) is now being used. So-called Big Data, routinely collected from a range of sources, including social platforms like Twitter, Flickr and Facebook (Barbosa et al., 2018) and most notably the explosion of mobile phone usage throughout the world, provides rich information on users' locations through time (Giannotti et al., 2011). Mobile network operators collect records of their users' calling patterns, a type of data called Call Detail Records (CDR), which include the location of the receiving tower where each voice call or text message is made, as well as the location of the recipient. Over time, each user's calling patterns can be used to reconstruct a detailed record of their location history. The collective mobility history of all users' movements through time provides insight on total population flows between all cellular network locations during any specified period of time. This enables the study of users' behaviors at very high spatiotemporal resolution over both local and system-level spatial scales at time scales of minutes to months to years (e.g. Song et al., 2010b). As each phone is embedded within an existing social fabric, CDR allow the analysis of the changing structure of social organization as people (i.e. individuals, social networks, communities, religious and ethnic groups, etc.) respond to a diversity of stimuli. CDR data has been used for urban planning (e.g. Becker et al., 2011), and to describe and evaluate commuting (e.g. Iqbal et al., 2014) and environmental displacement resulting from earthquakes and hurricanes (e.g. Lu et al., 2016, 2012). They have also been used to evaluate mobility as a vector for the spread of infectious diseases such as ebola (e.g. Wesolowski et al., 2014b; Balcan et al., 2009; Belik et al., 2011; Wesolowski et al., 2014a).

CDR data offer a vastly clearer and more detailed description of the communication and mobility behaviors of people as they go about their daily lives, compared to traditional data on human mobility, such as surveys and censuses, which are collected at relatively coarse time-scales, i.e. months and years (i.e. Bell and Ward, 2000). CDRs are compiled by network operators principally for the purposes of billing customers for their use of the network, not for scientific analysis; therefore, the main challenge with analyzing CDR is the size, complexity and richness of datasets. CDR are inherently high dimensional and noisy (Chen and Zhang, 2014), and quantitative analyses must incorporate dimensional reduction and denoising approaches. Once done, the remaining challenge is retrieving a relevant signal from the data at the appropriate spatial and temporal scale for each specific mobility pattern (Song et al., 2010b).

Here, we describe a data-driven approach to CDR analysis that explicitly addresses the multiscale nature of the mobility patterns embedded in the data and reflected in the system under study. We analyzed CDR from users of the Orange/Sonatel cellular network, collected in Senegal between 1 January and 31 December 2013 (see Fig. 1 for an illustration of mobility in Senegal for a given day). De-identified data entries included information on the time of the call, the mobile phone tower used and the duration of call. To identify and characterize different spatio-temporal modes of human mobility captured in CDR, we developed a novel computational approach based on spectral graph wavelets, an extension of classical wavelet analysis to the setting of networks. There are now numerous examples of where CDR data has been used to understand patterns of human mobility (e.g. Jarv et al., 2014; Calabrese et al., 2013; Dobra et al., 2015), including those that also explicitly address multiscale patterns (Phithakkitnukoon et al., 2012) using methods from statistical physics (e.g. Lambiotte et al., 2008; Simini et al., 2012). Here, we have made new mathematical advances to spectral graph wavelets to improve upon these state of the art approaches to the multiscale decomposition of CDR data. In doing so we were able to identify and characterize various multiscale spatio-temporal patterns of human mobility in Senegal for the year 2013.

To demonstrate the utility of our approach we focused on dynamic multiscale mobility patterns to/from a specific city in Senegal - Touba, a market town and religious center in Senegal's agricultural breadbasket. Our goal was to identify and characterize the different spatio-temporal patterns of human mobility that contrast in overall spatial scale and temporal duration. We focus on inter-city forms of mobility to/from Touba, including seasonal migration relating to changes in agriculture and a mobile labor force, as well as punctuated patterns relating to calendar festivals, local elections, or religious holidays. The identification and interpretation of these spatio-temporal scales and patterns of human mobility is of value to the ultimate goal of extracting key dynamics from complex adaptive systems in general.

95 METHODS

96 Human Mobility Data

97 To analyze the multiscale nature of human mobility, we developed a new approach to spectral graph
98 wavelets which we then applied to de-identified, pre-processed extracts of CDR from the Orange/Sonatel
99 mobile network in Senegal generated between January 1 and December 31, 2013. These data were

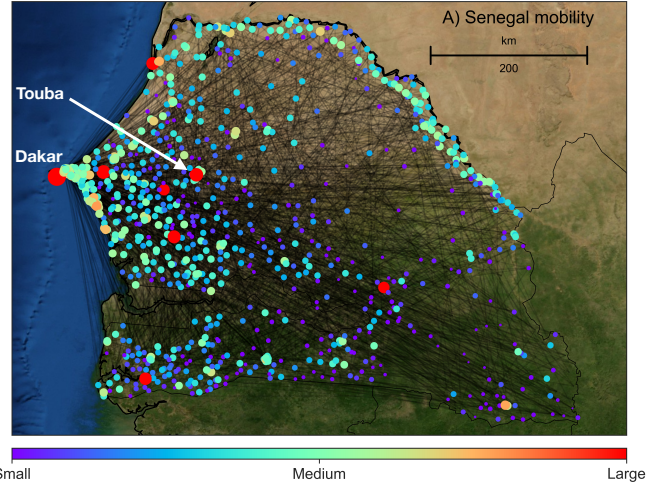


Figure 1. A) Map of Senegal with major cellular communication towers: these are the nodes in our human mobility networks. Nodes are color coded and sized by population density and edges connecting them highlight the density and complexity of human communication and mobility networks. These networks are changing over time, and in Senegal there are many large-scale mobility events, relating to religious events (often held at Touba, the focal city of this study) as well as to seasonal changes in weather and agriculture.

100 obtained from the Orange Telecom Data for Development Challenge (D4D) and are highly sensitive.
 101 As a consequence they cannot be made publicly available, but can be obtained by contacting Orange.
 102 These data include a number of variables on individual mobility behaviors/locations for 300,000 randomly
 103 sampled users on a rolling 2-week basis. These data were arranged into a pairwise origin-destination
 104 network whose vertices, or nodes, are cell towers and whose edges are weighted by the volume of
 105 phones moving/flowing between each tower pair for each 24-hour period over the entire year of 2013. To
 106 highlight inter-city mobility, we first aggregated the cell towers of key cities into single nodes, following
 107 administrative boundaries. Then, for each 24 hour period, a one was added to a given edge i, j if a phone
 108 moved from node i to node j . To further filter out intra-city mobility, repeated trips between the same
 109 towers for the same user within a 24-period were not counted. This effectively removes “double” trips,
 110 and leaves the one-way trips, for example home-work commutes. After all this, mobility was defined
 111 and quantified as an asymmetric affinity matrix A varying through time, where $A_{ij}(t)$ is the total number
 112 of unique trips made by users between towers i and j on day t of 2013 (see Fig. 1A for a geographic
 113 representation for one of these daily affinity matrices). In order to normalize the data so that the signal
 114 from high volume mobility in areas such as Dakar, the capital of Senegal, did not wash out all other
 115 signals, we calculated relative mobility by dividing the entries of $A(t)$, by their respective row sums.
 116 In this way the number of trips on a given day from a given node are now weighted by the amount of
 117 people moving from that node. In order to perform the SGW analysis, we then converted this asymmetric
 118 affinity matrix to a symmetric one by taking the average of two-way mobility patterns between pairs of
 119 cell-towers. Last, so as to not include intra-city traffic, we set the diagonal of A to zero. The result was a
 120 symmetric affinity matrix/network with zeros on the diagonal for every day of 2013.

121 **Multiscale Analysis using Spectral Graph Wavelets**

122 Networks of human mobility and communication are naturally modeled by graphs, sets of nodes connected
 123 by edges, each with an associated weight representing the strength of the connection. Here, higher edge
 124 weights indicate a greater flow of human migration between the edge’s two endpoints. Graphs can
 125 be viewed as discrete analogues of smooth objects such as geometric manifolds and surfaces, and the
 126 geometric content of these graphs is often analyzed using an associated Laplacian operator (Chung, 1997;
 127 Coifman and Lafon, 2006), as it encodes the structure of the graph in a natural way. In particular, its
 128 eigenfunctions can be used to construct a family of wavelets, which allows one to decompose functions in
 129 the same spirit as the indispensable Fourier analytic approach to time series analysis. This is the starting
 130 point of our study.

131 In Fourier analysis, one uses eigenfunctions $\{\phi_k\}$ of the Laplacian as basis vectors and their associated
 132 eigenvalues $\{\lambda_k\}$ inform us of the functions' features: larger eigenvalues are associated to higher frequency
 133 or, equivalently, smaller scale variations, and lower eigenvalues correspond to the large-scale features.
 134 These functions ϕ_k are, however, supported across the entire domain in question, and so a function's
 135 Fourier coefficients $c_k = \langle \phi_k, f \rangle$, integrate features from disparate regions in the domain. Wavelet families,
 136 on the other hand, allow one to perform a similar analysis while restricting attention to a local region
 137 defined by a central point and a scale, or radius.

138 Given that human mobility networks are inherently multiscale as well as highly heterogeneous, a
 139 method is required that is both multiscale and localized. In the classical settings of time series analysis
 140 and image analysis, wavelets were developed to exhibit precisely these two traits. Here we employed
 141 a generalization of wavelets to graphs, called spectral graph wavelets. Spectral graph wavelets have
 142 been previously used to study human mobility, for example automobile traffic (Mohan et al., 2014), in
 143 analyzing human mobility from photo activity via Flickr (Dong et al., 2013), and in general clustering and
 144 community detection (Tremblay and Borgnat, 2013).

145 An important first choice to make when employing spectral graph wavelets is the shape of the wavelet
 146 to be used, or in other words the "wavelet kernel". This can have a profound effect on the analysis. In
 147 particular, we employed a wavelet kernel based specifically on the heat kernel yielding what we call
 148 Hermitian Graph Wavelets (for details of the mathematical analysis see: Gelbaum et al., 2019), which
 149 allows us to associate explicit radii to the wavelets rather than a scale parameter that is independent of
 150 any metric on the graph. By using these wavelets, we were able to produce a data analysis method that
 151 efficiently extracted key geometric information from the time-varying human mobility networks $A(t)$.

152 This approach provides a decomposition whose components may be ordered by importance. Whereas
 153 in a Fourier decomposition the largest coefficients c_k indicate the eigenfunctions which contain most of
 154 the original function's information, in the present study the norm of the wavelet gives a measure of the
 155 gross data encoded by it. The outputs of this analysis are a set of wavelet functions associated to each
 156 vertex (i.e. for every cell tower in Senegal), as well as a single *dominant scale* for each vertex representing
 157 the scale containing the most information for that vertex. By fixing a choice of vertex and observing how
 158 the wavelet at the dominant scale evolves over time we have a vastly simplified geometric summary of
 159 how the graph structure is changing near the focal vertex. As a result, these wavelet functions are rich in
 160 multiscale geometric content, and we used them to identify and characterize different forms or modes of
 161 human mobility that occur throughout Senegal over the year 2013.

162 Applying Spectral Graph Wavelets to Mobility Networks

Given the set of daily affinity matrices, $A(t)$, the application of Spectral Graph Wavelets is as follows.
 First, for each of the daily affinity matrices, we constructed their associated Laplacian matrices:

$$\Delta(t) = D(t) - A(t),$$

where $D(t)_{ii} = \sum_j (A(t))_{i,j}$ and $D(t)_{ij} = 0$ for $i \neq j$. Once done, the eigenvectors and eigenvalues of $\Delta(t)$,
 $\{\phi_{k,t}\}$ and $\{\lambda_{k,t}\}$ respectively, were then computed. Then, Hermitian graph wavelets were formed as:

$$\psi_{s,x}(y) = \sum_k s \lambda_k(t) e^{-s\lambda_k(t)} \phi_{k,t}(x) \phi_{k,t}(y), \quad (1)$$

for a chosen set of scales $s \in \{s_n\}$ (note that $\psi_{s,x}(y) = \psi_{s,y}(x)$). These functions exhibit several properties
 that make them ideal for decomposing signals measured on large and complex networks: they are localized,
 in that they provide information for every node, and the power of each wavelet (i.e. its norm, as a vector)
 gives us a measure of its importance with respect to the global network structure (Gelbaum et al., 2019).
 This is analogous to classical Fourier analysis where large Fourier coefficients in the decomposition of a
 function indicate the major modes comprising the function. Rather than forming an orthonormal set, the
 wavelet functions $\{\psi_{s_n,x}\}$ form a *frame* and rather than the classical Parseval equality, an approximate
 Parseval equality holds: for a function f on the network there are constants $0 < B < C < \infty$ with

$$B \|f\|^2 \leq \sum_{s_n,x} |\langle f, \psi_{s_n,x} \rangle|^2 \leq C \|f\|^2,$$

where

$$\|f\|^2 = \sum_x |f(x)|^2,$$

with the sum taken over all nodes x in the network. The values of B and C depend both on choice of wavelet kernel and the scales chosen. It is always possible to choose scales and (by renormalizing if necessary) achieve a frame with the values of B and C as close to 1 as desired (i.e. Hammond et al., 2011). The determination of the scales $\{s_n\}$ input into the algorithm is largely ad hoc and some trial and error is required. While it is up to the investigator to make this choice, some general points can be made: the chosen scales should always be positive and the largest should not be too much bigger than the largest eigenvalue. The goal is to get a good partitioning of the interval $[0, \max\{\lambda(t)\}]$ relative to the spacing of the eigenvalues, but as the eigenvalues are in general not uniformly spaced some experimentation may be required to find the resolution that is most informative. Having a well distributed set of scales will also ensure that the calculation of wavelet power is not sensitive to small changes in the network's structure or the specific scales chosen. In other words, calculations will be stable.

With an appropriately chosen set of scales, if we let f be a delta function at node z , $f = \delta_z$ (meaning $f(z) = 1$ and $f(x) = 0$ for all other nodes $x \neq z$), the above Parseval bounds and $\psi_{s,x}(y) = \psi_{s,y}(x)$ symmetry imply that

$$1 = \|f\|^2 \approx \sum_{s_n, x} |\langle f, \psi_{s_n, x} \rangle|^2 = \sum_{s_n} \sum_x |\psi_{s_n, z}(x)|^2 = \sum_{s_n} \|\psi_{s_n, z}\|^2.$$

Thus the values of $\|\psi_{s_n, z}\|^2$ serve to indicate the relative importance of each scale with respect to the vertex z . In this way, large values of $\|\psi_{s_n, z}\|^2$ correspond to the major scales of importance at the node z . We utilize this intuition and define the dominant scale at each vertex to be

$$S(z, t) = \arg \max_{s_n} \|\psi_{s_n, z}\|^2. \quad (2)$$

This measures the scale at which a given vertex is most well-connected to the rest of the network.

The above Hermitian graph wavelet functions yield a multiscale analysis at each vertex in the graph (i.e. for every cell tower in Senegal). To highlight the ability of spectral graph wavelets to identify multiscale patterns, we chose to build our wavelets with a fixed base point at the vertex corresponding to the city of Touba (denoted x_T), and track the scale of the dominant wavelet function $S(x_T, t)$ as above, through time. We abbreviate this as $S(t)$. We thus obtain a sequence of dominant wavelet functions on the network $\psi_{S(t), x_T}(t, y)$, where the first argument indicates the dependence on the changing network structure encoded in $A(t)$ and the second argument y corresponds to vertices of the graph on which the function takes its values.

RESULTS

To demonstrate the utility of spectral graph wavelets for identifying the main spatio-temporal scales and patterns of human mobility, we calculated dominant wavelet functions centered on Touba, the market city in Senegal's central breadbasket and an important site for religious festivals, and compared results with those produced from a basic analysis of the original population flow data. More specifically, for any given day, human mobility to/from a given location can be extracted from the mobility matrices $A(t)$ and visually inspected (Fig. 2A). Doing so for Touba, one finds that large cities such as Dakar on the west coast account for most of the total daily flow in and out of Touba (i.e. compare the location of large red nodes in Fig. 2A).

In contrast, Fig. 2B depicts the dominant wavelet function for the same day as plotted in Fig. 2A. The function $\psi_{S(t), x_T}(t, y)$ reveals a distinct spatial pattern, with a large positive value centered on Touba, that rapidly diminishes to negative values in surrounding nodes, before approaching zero at geographically remote nodes. We note that despite the fact that the wavelet function was calculated using only the population flow data, and not any explicit spatial distance between location pairs, the dependence of human traffic on the distance traveled (i.e. the proximity of Touba to other locations) is apparent in the resulting wavelet function. In other words, we are observing a strong spatial autocorrelation in human mobility levels, which is both intuitive and expected.

To characterize changes in human mobility through time, focusing on Touba, we first examined changes in the total traffic to/from Touba over time (Fig. 3A); this is calculated by summing the mobility values to/from Touba at all locations for each day (i.e. taking a row-sum of a given affinity matrix $A(t)$). \log_{10} total mobility to/from Touba over time reveals a variety of qualitative features, most striking is a

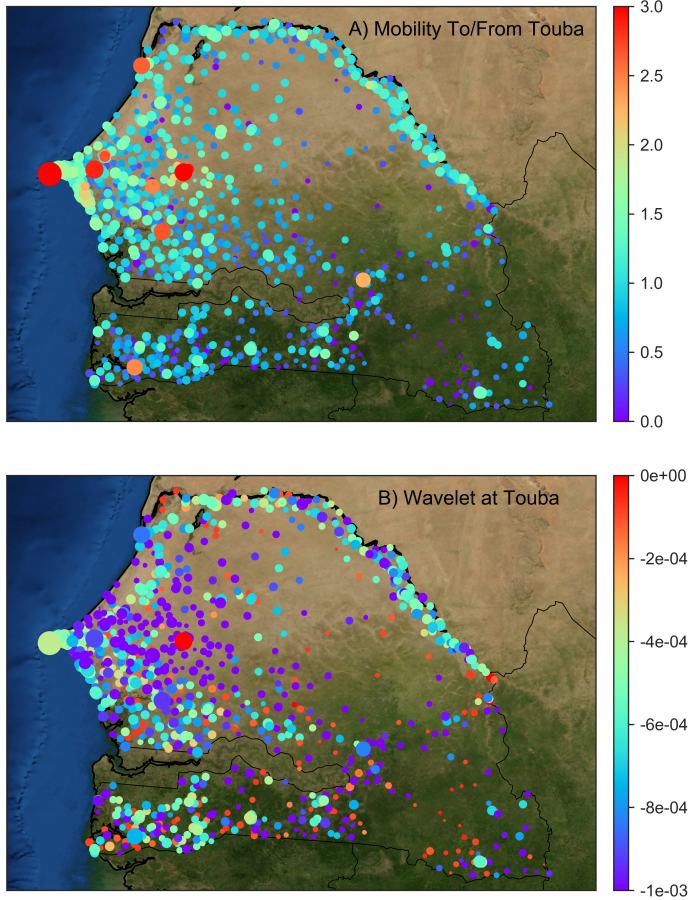


Figure 2. A) Cell-towers (i.e. human mobility nodes) in Senegal color coded by the \log_{10} number of people moving to/from Touba on a random day in 2013, and sized by local population density. B) In contrast, colors now denote the dominant wavelet function centered on Touba for the same day. Here, node size remains proportional to local population density. The two maps reveal very different information. In (A) mobility to/from the major urban hubs, such as Dakar the capital, are identified and in (B) the shape of the dominant wavelet function is highlighted: wavelet function values are positive at Touba (the large red node near the center of Senegal) decreasing to large negative values in nearby towns, before becoming less negative at far-off towns).

204 large peak in traffic corresponding to the commemoration of Touba's mosque's 50th anniversary, which
 205 occurred May 30th, 2013 (day 150), as well as the end of Ramadan August 7th, 2013 (day 219) and Eid
 206 al-Adha on October 15 (day 287).

207 We then clustered days based upon origin-destination flow values in $A(t)$. For each day the vector
 208 of mobility values to/from Touba were extracted from the mobility matrices $A(t)$. We clustered days
 209 based on these values, using the Louvain method for community detection (Blondel et al., 2008). This
 210 involved calculating the Euclidean distance between days based on their mobility values, and running
 211 the algorithm numerous times because it is non-deterministic. We chose the Louvain method primarily
 212 because it provides an objective determination of the number of clusters. This is in contrast to other
 213 common clustering approaches which require the number of clusters to be chosen (e.g. k-means). A
 214 sensitivity test of the Louvain method, as well as other community detection / clustering approaches is
 215 provided in the Supplementary Material.

216 Clustering these mobility data for Touba identified two main time periods, corresponding to seasonal
 217 changes in the Senegalese weather and agriculture, as the rainy season begins around September. There is
 218 a third cluster corresponding to a short intermediate period (see Fig. 3A, changes in the marker color:

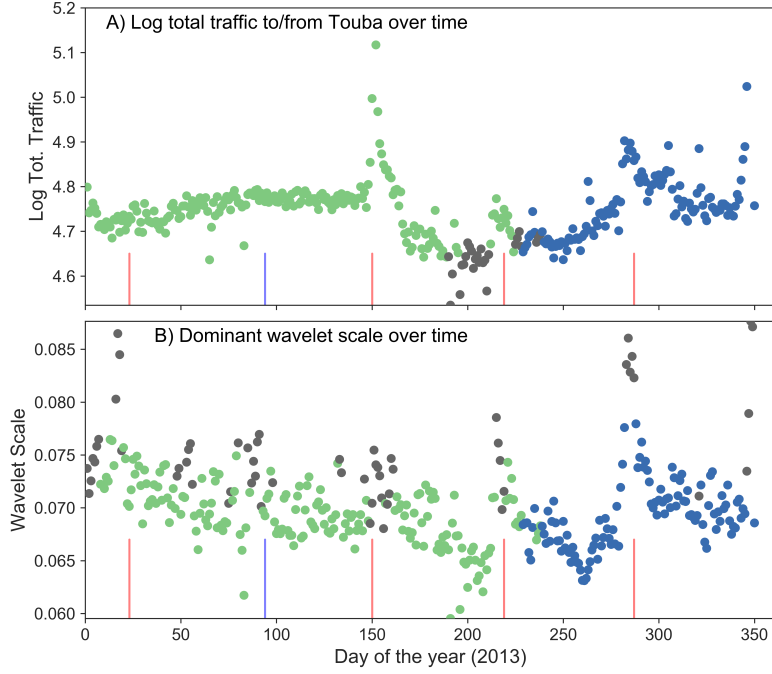


Figure 3. A) Time-series of the \log_{10} total mobility to/from Touba for 2013, colored by group ID produced from clustering days based on their mobility values. This cluster analysis identifies mobility associated with the dry (green) and wet (blue) seasons (with an transitional phase in grey), and there are peaks in total traffic to/from Touba that correspond with major religious events at day 150, 219 and 287; however, the cluster analysis does not recognize these events as distinct. B) In contrast, changes over time in the scale associated with the dominant wavelet function (centered on Touba) better reveals the punctuated and large-scale mobility events related to religious celebrations (vertical red lines) and Senegal's independence day (blue vertical line). In addition, using these dominant wavelet functions to cluster days extracts meaningful information about seasonal migration (points in green and blue), as well as the short-term / large-spatial scale events (points in grey).

219 green, grey and blue correspond to the dry, intermediate and wet seasons respectively). Interestingly,
 220 the clustering only picked out these long-term changes in mobility, and not the short-punctuated events
 221 relating to religious festivals or political events. This is because while these kinds of short-term events are
 222 associated with a change in total traffic to/from Touba, any topological changes in the inter-city traffic
 223 profile are obscured by the complexity and irregularity of the data.

224 In contrast to these results created by analyzing the raw mobility values, clustering dominant wavelet
 225 functions over time revealed more nuanced information about mobility in Senegal in 2013. Clustering
 226 was done using $\psi_{S(t),x_T}(t,y)$ in place of population flow values: we calculated the Euclidean distance
 227 between daily pairs of Touba-centered wavelet functions, before using the Louvain community detection
 228 algorithm to identify clusters. Like the analysis of the relative population flow values described above,
 229 this clustering of daily wavelet functions identifies changes in human mobility relating to the dry and
 230 wet season. Importantly however, now the presence of relatively short-term and large-scale events were
 231 identified throughout the year. These events are marked by a short-term widening of the wavelet function
 232 centered on Touba (in network space), and correspond to the three religious migration events listed above.
 233 In addition, other events are identified: the Maouloud/Gamou celebration that occurred on January 23,
 234 2013 (day 23) and Independence Day that occurred April 4th, 2013 (day 94). There are two extra events
 235 that this clustering approach identified, around day 50 and at the end of the year. The former is an
 236 unknown event; the authors do not know of any political, religious, or cultural gathering that occurred
 237 near Touba at that time, though we note that the absence of evidence is not evidence of absence. Indeed,
 238 the similarity of the network structure at day 50 to that of other verified major migrations is a strong
 239 motivator for further investigation. The latter date, at the end of the year, is likely associated with

240 new-years celebrations/holidays. Crucially, the total traffic to/from Touba does not change during many
 241 of these events, and they are not identified by clustering the relative population flow data; the scale of the
 242 dominant wavelet functions fluctuate due to changes in connectivity within the network and this manages
 243 to distinguish between typical traffic patterns and migration events.

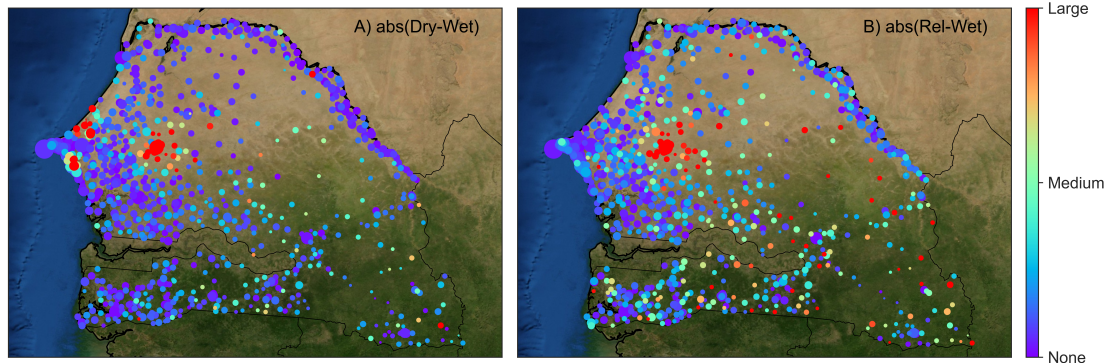


Figure 4. Main spatio-temporal patterns of human mobility can be identified by averaging the dominant wavelet functions associated with the cluster groups shown in Fig. 3B. Then, these modes of human mobility can be compared by calculating their absolute difference and plotting as a map. A) The absolute difference in the average dominant wavelet function (centered on Touba) associated with the dry and wet seasons highlights changes in mobility to/from the coast and Touba. B) The absolute difference in the average wavelet function (centered on Touba) associated with religious events and the wet season reveals changes in mobility in far-off towns in the east of Senegal, and Touba.

244 Averaging the daily wavelet functions associated with each cluster (i.e. producing an average dominant
 245 wavelet function centered on Touba for the dry and wet seasons, and for each short-term / large-scale
 246 event) reveals stark spatial differences (Fig. 4). For example, the absolute difference between the average
 247 wavelet function relating to the dry and wet seasons (Fig. 4A) identifies change in several coastal towns
 248 (along with changes in mobility in and around Touba). These changes reflect two processes. First, in
 249 Senegal there is a large and mobile agricultural work-force. Seasonally employed farm laborers from
 250 the coast use Touba as a stepping stone to rural locations in the interior of the country. Second and also
 251 associated with the start of the rainy season are floods, and in 2013 the coast experienced significant
 252 flooding. These differences in the average wavelet functions associated with the dry and wet clusters also
 253 reflect the impact of the floods on human mobility.

254 Additional nuances emerge in the punctuated modes of mobility associated with the religious festivals
 255 noted earlier. In contrast to the seasonal changes in mobility, the absolute difference between the average
 256 wavelet function associated with short-term / large-scale events, in this case Eid al-Adha on October 15
 257 (day 287), and the wet season identifies change in mobility to/from many small rural towns in the far
 258 east of Senegal (Fig. 4B). These differences in average dominant wavelet functions clearly identify the
 259 long-distance travel that people make as they go to/from Touba for the religious event.

260 This kind of geographically meaningful information can be used to explore differences in the various
 261 modes of human mobility found by clustering daily wavelet functions. In general, this approach more
 262 readily reveals heterogenous spatial and network features, relative to results produced from the analysis of
 263 the relative population mobility values, which simply described major seasonal changes in flows to/from
 264 Touba. Importantly, it bears noting that while we present results from Touba, the spectral graph wavelet
 265 analysis also characterizes the main spatio-temporal scales and patterns of human mobility *for every*
 266 *node within the network*. Hence, while we have demonstrated its utility with regards to Touba, there is
 267 additional spatially meaningful information that we did not show or analyze.

268 DISCUSSION

269 To improve upon current abilities to characterize changes in human mobility over time we developed and
 270 applied a new manifold learning method based on spectral graph wavelets (i.e. Hermitian graph wavelets)
 271 to a CDR dataset. These data describe the origin-destination mobility patterns for people living in Senegal,

272 daily for the year 2013. Our approach is non-linear, localized and scale explicit, that is it can be used
273 to identify multiscale patterns of human mobility for each node in a mobility network. This is key to
274 disentangling multiscale patterns with big and rich datasets like those produced by CDRs. Spectral graph
275 wavelets applied to these data allowed us to identify seasonal changes in Senegalese human mobility,
276 as well as punctuated large-scale events relating to religious migration and a national holiday. These
277 short-term but large-spatial-scale events were not identified by a standard approach applied to the original
278 mobility values themselves (i.e. $A(t)$), because these data contained too much noise. As a consequence,
279 our spectral graph wavelets approach provides a new method for the multiscale decomposition of human
280 mobility data, and expands the utility of CDR data for anticipating and preparing for changes in human
281 mobility.

282 Identifying the main spatio-temporal scale and patterns of human mobility, and the spatio-temporal
283 scales at which they occur, is an important part of developing policies for a whole host of operations,
284 ranging from traffic infrastructure to disaster response planning (Jiang et al., 2017). These kinds of spatial
285 policies have previously been made using far coarser data, both spatially and temporally (e.g. Bell and
286 Ward, 2000). Here, making use of relatively high resolution CDR data, we were able to tease out the
287 spatial signal of punctuated large-scale events, in contrast to a standard approach applied to data on
288 population flow values. The rate at which new data is created – always at higher temporal frequency and
289 greater spatial resolution – is ever growing, and the quantitative tools used to extract useful information
290 from monthly or even annual datasets are rapidly diminishing in utility (Lee and Kang, 2015). For the
291 best use of these new data (i.e. next-gen CDR datasets) new tools are required, and indeed, new tools that
292 can articulate the complex and adaptive nature of human mobility have extreme utility (e.g. Scheffer et al.,
293 2018). Like human mobility, other complex adaptive systems are multiscale by nature (Levin, 1998), and
294 in general there is a growing need to extract information about the micro-scale agents that comprise these
295 systems, from which meso- and macro-scale patterns emerge (Folke, 2006). Data-analytic tools designed
296 with the multiscale nature of complex adaptive systems in mind will help policy makers develop plans that
297 explicitly account for the emergence of patterns over a continuum of scales, like in this case the various
298 modes of human mobility in Senegal, and their associated network/geographic scale.

299 The use of spectral graph wavelets allowed us to essentially transform the origin-destination mobility
300 data (i.e. $A(t)$) to a form that better highlights the differences of human mobility patterns. In that spirit,
301 this analysis can be thought of as a process of dimensional reduction or a denoising of the raw data,
302 in a manner that accounts explicitly for network scale. Analyzing the mobility data did not provide
303 the same kinds of scale-dependent information because it is noisy. Admittedly, when analyzing the
304 mobility matrices $A(t)$ we used a very basic approach to classification. There are indeed many other
305 more sophisticated approaches that we could have been employed, in order to contrast with the results
306 produced from analysis of the dominant wavelets functions. These approaches vary from traditional
307 dimensional reduction techniques that rely on linear correlations, such as Principal Components Analysis
308 (PCA), to machine learning approaches for feature identification (e.g. Bi et al., 2003). Indeed, we see that
309 there is a great opportunity for using the wavelet transformed data in combination with machine learning
310 approaches to classification and feature extraction.

311 The multiscale and localized information that spectral graph wavelets provides can be used in many
312 other ways. Here, we have analyzed human mobility information gained from the CDR data, but the CDR
313 dataset can also be used to construct human communication networks through time. Performing the same
314 analysis on both sets of data would produce concurrent wavelet functions through time. A comparison
315 of changes in the main spatio-temporal scales and models of human communication and mobility might
316 reveal early-warning signals of migration/displacement. Simply put, as people prepare to move they are
317 likely to call their ultimate destination, and this information can help policy makers prepare for changes
318 in population density at specific nodes/places. There is an opportunity to utilize methods from manifold
319 matching (e.g. Shen et al., 2017) to make these comparisons. Manifold matching has been used in image
320 recognition to match photos of the same person, for example. Here, instead of a set of photos from a
321 person's face, the manifolds that would be compared are those associated with a complex system (the
322 Senegal cellular network) described in two ways (i.e. communications and mobility).

323 Early detection of large-scale human migration is evident in our analysis. For example in Fig. 3B,
324 the days with large wavelet scale (i.e. the grey dots) often precede the date of the event (i.e. the vertical
325 red lines). This suggest that our method could provide quantitative measures of “anomalous” mobility
326 patterns associated with these events. For example, one could compare a given day’s dominant wavelet

327 function with those from an average wavelet function constructed from the preceding week or month.
328 This is similar to, but contrasts with, what we have done here comparing seasonal patterns of mobility. In
329 doing so, one could compute how anomalous a given day is relative to recent times. This approach to
330 anomaly detection is common, but the use of our HGW method to predict unknown oncoming events
331 from CDR data would be novel.

332 Additional early-warning signals of mass human-mobility can also be sought from the dynamics inher-
333 ent to mobility networks alone. These kinds of early-warning signals come from dynamical systems and
334 bifurcation theory (Scheffer et al., 2009) and are measured by changes in the variance and autocorrelation
335 in macroscopic variables (Boettiger et al., 2013), for example changes in the density of people in a certain
336 neighborhood. For human mobility CDR data, there is an opportunity to advance new early-warning
337 signals of multiscale change using manifold learning. Specifically, spectral graph wavelets is one way
338 to learn changes in the geometry of the manifold on which dynamics occur, but there are others, for
339 example diffusion maps (Coifman and Lafon, 2006) and Laplacian eigenmaps (Belkin and Niyogi, 2003).
340 Systems undergoing a bifurcation driven by some macroscopic variable should *a fortiori* exhibit changes
341 in geometry at small and intermediate scales as well; a multiscale analysis may then allow one to directly
342 address how these kinds of large and abrupt changes in complex systems are related to changes in the
343 behavior of micro-scale agents (i.e. in this case, how individual people move from place to place).

344 Identifying the main spatio-temporal scales and patterns of human mobility, and potentially early-
345 warning signals of changes between them, is of principal interest of groups tasked with managing human
346 communities (Jiang et al., 2017), as they go about their everyday lives as well as respond to infrequent
347 but impactful events like a natural hazard. In Senegal, flooding is a persistent problem and indeed in
348 2013 the capital Dakar was severely hit. These kinds of events can lead to the permanent displacement
349 of people from their homes, and similarly to identifying the main spatio-temporal scales and patterns of
350 human mobility as done here, there is value to identifying where and when this displacement occurs (Xie
351 et al., 2016). Indeed, displacement is not necessarily instantaneous with regards to the perturbation, but it
352 may take a relatively long time for people to “realize” their displacement (Black et al., 2013). Multiscale
353 methods like spectral graph wavelets applied to CDR data can help distinguish these additional modes of
354 human mobility, and further, methods from manifold matching are likely to be useful too.

355 In sum, we have made advances to spectral graph wavelets (specifically Hermitian graph wavelets)
356 for analyzing CDR human mobility data. Our approach extracts useful information that is localized and
357 scale-explicit, and we identified seasonal changes in human mobility as well as punctuated large-scale
358 mobility events associated with religious celebrations and a national holiday. Here, we focused our
359 multiscale analysis on one place in Senegal - Touba - a place of religious significance. However, the
360 spectral graph wavelets analysis produces information for all nodes in the network, and there is rich vein
361 of scale-explicit information in the full wavelet transform of the origin-destination mobility data. Last,
362 while the growth in data obtained for complex adaptive systems is daunting (Scheffer et al., 2009), there
363 are opportunities to employ new localized and scale-explicit dimensional reduction techniques, like we
364 have done so here, to greatly improve our ability to characterize and predict multiscale change. This
365 ability is vital if we are to maintain welfare from the complex systems in which we are embedded.

366 REFERENCES

- 367 Balcan, D., Colizza, V., Gonçalves, B., Hu, H., Ramasco, J. J., and Vespignani, A. (2009). Multiscale
368 mobility networks and the spatial spreading of infectious diseases. *Proceedings of the National
369 Academy of Sciences*, 106:21484–21489.
- 370 Barbosa, H., Barthelemy, M., Ghoshal, G., James, C. R., Lenormand, M., Louail, T., Menezes, R.,
371 Ramasco, J. J., Simini, F., and Tomasini, M. (2018). Human mobility: Models and applications.
372 *Physics Reports*, 734:1–74.
- 373 Becker, R. A., Caceres, R., Hanson, K., Loh, J. M., Urbanek, S., Varshavsky, A., and Volinsky, C.
374 (2011). A tale of one city: Using cellular network data for urban planning. *IEEE Pervasive Computing*,
375 10(4):18–26.
- 376 Belik, V., Geisel, T., and Brockmann, D. (2011). Natural human mobility patterns and spatial spread of
377 infectious diseases. *Physical Review X*, 1(1):011001.
- 378 Belkin, M. and Niyogi, P. (2003). Laplacian eigenmaps for dimensionality reduction and data representa-
379 tion. *Neural computation*, 15(6):1373–1396.

- 380 Bell, M. and Ward, G. (2000). Comparing temporary mobility with permanent migration. *Tourism
381 Geographies*, 2(1):87–107.
- 382 Bi, J., Bennett, K., Embrechts, M., Breneman, C., and Song, M. (2003). Dimensionality reduction via
383 sparse support vector machines. *Journal of Machine Learning Research*, 3(Mar):1229–1243.
- 384 Black, R., Arnell, N. W., Adger, W. N., Thomas, D., and Geddes, A. (2013). Migration, immobility and
385 displacement outcomes following extreme events. *Environmental Science & Policy*, 27:S32–S43.
- 386 Blondel, V. D., Guillaume, J.-L., Lambiotte, R., and Lefebvre, E. (2008). Fast unfolding of communities
387 in large networks. *Journal of statistical mechanics: theory and experiment*, 2008(10):P10008.
- 388 Boettiger, C., Ross, N., and Hastings, A. (2013). Early warning signals: the charted and uncharted
389 territories. *Theoretical ecology*, 6(3):255–264.
- 390 Calabrese, F., Diao, M., Lorenzo, G. D., Ferreira, J., and Ratti, C. (2013). Understanding individual
391 mobility patterns from urban sensing data: A mobile phone trace example. *Transportation Research
392 Part C: Emerging Technologies*, 26:301 – 313.
- 393 Chen, C. P. and Zhang, C.-Y. (2014). Data-intensive applications, challenges, techniques and technologies:
394 A survey on big data. *Information Sciences*, 275:314–347.
- 395 Chung, F. R. K. (1997). *Spectral graph theory*, volume 92 of *CBMS Regional Conference Series in
396 Mathematics*. Published for the Conference Board of the Mathematical Sciences, Washington, DC; by
397 the American Mathematical Society, Providence, RI.
- 398 Coifman, R. R. and Lafon, S. (2006). Diffusion maps. *Appl. Comput. Harmon. Anal.*, 21(1):5–30.
- 399 Dobra, A., Williams, N. E., and Eagle, N. (2015). Spatiotemporal detection of unusual human population
400 behavior using mobile phone data. *PLOS ONE*, 10(3):1–20.
- 401 Dong, X., Ortega, A., Frossard, P., and Vandergheynst, P. (2013). Inference of mobility patterns via
402 spectral graph wavelets. In *2013 IEEE International Conference on Acoustics, Speech and Signal
403 Processing*, pages 3118–3122.
- 404 Folke, C. (2006). Resilience: The emergence of a perspective for social–ecological systems analyses.
405 *Global environmental change*, 16(3):253–267.
- 406 Gelbaum, Z., Titus, M., and Watson, J. (2019). Multi-scale analysis on complex networks using hermitian
407 graph wavelets. *arXiv*, arXiv:1901.07051.
- 408 Giannotti, F., Nanni, M., Pedreschi, D., Pinelli, F., Renso, C., Rinzivillo, S., and Trasarti, R. (2011).
409 Unveiling the complexity of human mobility by querying and mining massive trajectory data. *The
410 International Journal on Very Large Data Bases*, 20(5):695–719.
- 411 Hammond, D. K., Vandergheynst, P., and Gribonval, R. (2011). Wavelets on graphs via spectral graph
412 theory. *Appl. Comput. Harmon. Anal.*, 30(2):129–150.
- 413 Iqbal, M. S., Choudhury, C. F., Wang, P., and Gonzalez, M. C. (2014). Development of original destination
414 matrices using mobile phone call data. *Transportation Research Part C: Emerging Technologies*, 40:63
415 – 74.
- 416 Jarv, O., Ahas, R., and Witlox, F. (2014). Understanding monthly variability in human activity spaces: A
417 twelve-month study using mobile phone call detail records. *Transportation Research Part C: Emerging
418 Technologies*, 38:122 – 135.
- 419 Jiang, S., Ferreira, J., and Gonzalez, M. C. (2017). Activity-based human mobility patterns inferred from
420 mobile phone data: A case study of singapore. *IEEE Transactions on Big Data*, 3(2):208–219.
- 421 Lambiotte, R., Blondel, V. D., de Kerchove, C., Huens, E., Prieur, C., Smoreda, Z., and Dooren, P. V.
422 (2008). Geographical dispersal of mobile communication networks. *Physica A: Statistical Mechanics
423 and its Applications*, 387(21):5317 – 5325.
- 424 Lee, J.-G. and Kang, M. (2015). Geospatial big data: challenges and opportunities. *Big Data Research*,
425 2(2):74–81.
- 426 Levin, S. A. (1998). Ecosystems and the biosphere as complex adaptive systems. *Ecosystems*, 1(5):431–
427 436.
- 428 Lu, X., Bengtsson, L., and Holme, P. (2012). Predictability of population displacement after the 2010
429 haiti earthquake. *Proceedings of the National Academy of Sciences*, 109(29):11576–11581.
- 430 Lu, X., Wrathall, D. J., SundsÅzy, P. R., Nadiruzzaman, M., Wetter, E., Iqbal, A., Qureshi, T., Tatem, A.,
431 Canright, G., Engaz-Monsen, K., and Bengtsson, L. (2016). Unveiling hidden migration and mobility
432 patterns in climate stressed regions: A longitudinal study of six million anonymous mobile phone users
433 in bangladesh. *Global Environmental Change*, 38:1 – 7.
- 434 Mohan, D. M., Asif, M. T., Mitrovic, N., Dauwels, J., and Jaillet, P. (2014). Wavelets on graphs

- 435 with application to transportation networks. In *17th International IEEE Conference on Intelligent*
436 *Transportation Systems (ITSC)*, pages 1707–1712.
- 437 Phithakkitnukoon, S., Smoreda, Z., and Olivier, P. (2012). Socio-geography of human mobility: A study
438 using longitudinal mobile phone data. *PLOS ONE*, 7(6):1–9.
- 439 Scheffer, M., Bascompte, J., Brock, W. A., Brovkin, V., Carpenter, S. R., Dakos, V., Held, H., Van Nes,
440 E. H., Rietkerk, M., and Sugihara, G. (2009). Early-warning signals for critical transitions. *Nature*,
441 461(7260):53.
- 442 Scheffer, M., Bolhuis, J. E., Borsboom, D., Buchman, T. G., Gijzel, S. M. W., Goulson, D., Kammenga,
443 J. E., Kemp, B., van de Leemput, I. A., Levin, S., Martin, C. M., Melis, R. J. F., van Nes, E. H.,
444 Romero, L. M., and Olde Rikkert, M. G. M. (2018). Quantifying resilience of humans and other
445 animals. *Proceedings of the National Academy of Sciences*, 115(47):11883–11890.
- 446 Shen, C., Vogelstein, J. T., and Priebe, C. E. (2017). Manifold matching using shortest-path distance and
447 joint neighborhood selection. *Pattern Recognition Letters*, 92:41–48.
- 448 Simini, F., Gonzalez, M. C., Maritan, A., and Barabasi, A.-L. (2012). A universal model for mobility and
449 migration patterns. *Nature*, 484(7392):96.
- 450 Song, C., Koren, T., Wang, P., and Barabasi, A.-L. (2010a). Modelling the scaling properties of human
451 mobility. *Nature Physics*, 6(10):818.
- 452 Song, C., Qu, Z., Blumm, N., and Barabasi, A.-L. (2010b). Limits of predictability in human mobility.
453 *Science*, 327(5968):1018–1021.
- 454 Tremblay, N. and Borgnat, P. (2013). Multiscale community mining in networks using spectral graph
455 wavelets. In *21st European Signal Processing Conference (EUSIPCO 2013)*, pages 1–5.
- 456 Wesolowski, A., Buckee, C. O., Bengtsson, L., Wetter, E., Lu, X., and Tatem, A. J. (2014a). Commentary:
457 containing the ebola outbreak - the potential and challenge of mobile network data. *PLoS Currents*,
458 6:1–20.
- 459 Wesolowski, A., Stresman, G., Eagle, N., Stevenson, J., Owaga, C., Marube, E., Bousema, T., Drakeley,
460 C., Cox, J., and Buckee, C. O. (2014b). Quantifying travel behavior for infectious disease research: a
461 comparison of data from surveys and mobile phones. *Scientific Reports*, 4:1–7.
- 462 Widhalm, P., Yang, Y., Ulm, M., Athavale, S., and Gonzalez, M. C. (2015). Discovering urban activity
463 patterns in cell phone data. *Transportation*, 42(4):597–623.
- 464 Xie, M., Neal, J., Burke, M., Lobell, D., and Ermon, S. (2016). Transfer learning from deep features for
465 remote sensing and poverty mapping. *arXiv*, arXiv:1510.00098.